

## Numerical Study of Inverted Shell Footing Behavior on Sandy Soil

Alaa Yousef Mahmood, Amina Ahmed Khalil \*

Department of Civil Engineering, College of Engineering, University of Mosul, Mosul, Iraq

### ARTICLE INFO

#### Article history:

Received June 30, 2023

Revised October 22, 2023

Accepted November 20, 2023

Available online December 10, 2023

#### Keywords:

Shell footing

Inverted shell

Upright shell

Settlement factor

Efficiency

### ABSTRACT

Inverted and upright shell foundations, are increasingly utilized in engineering projects as structural elements beneath buildings, towers, curved dams, and other structures. They serve as economical alternatives to shallow foundations when encountering high loads transmitted through weak soil. The purpose of this research is to use the numerical modeling program Midas GTS NX to better understand the load-settlement behavior of inverted shell footings subjected to vertically applied loads. The study involved variables related to the properties of shell cross-sections, embedment depth of footing, and angle of side slope of footing. Also, the shell efficiency factor and the non-dimensional settlement factor for the shell footing are studied. The results show that inverted shell footings exhibit higher load-carrying capacity compared to traditional flat footings. Furthermore, it was found that inverted shell footings within the range of side slope angles of  $15^{\circ}$ – $30^{\circ}$  have a higher load-carrying capacity than traditional flat footings. Additionally, an increase in embedment depth was shown to be effective in enhancing the load-carrying capacity of inverted shell footings. From the obtained results, it was also concluded that the shell efficiency factor ( $\eta$ ) of inverted shell footings is high. In particular, the inverted pyramid shell footing with an angle of  $15^{\circ}$ – $30^{\circ}$  exhibited higher efficiency compared to other footings, by 48.3% and 39.8%, respectively. The settlement improvement factor ( $F_s$ ) of inverted shell footings was found to be low with the inverted pyramid shell footing at an angle of  $15^{\circ}$ – $30^{\circ}$  having a lower value compared to others by  $5 \times 10^{-4}$  and  $507 \times 10^{-4}$ , respectively.

\* Corresponding author.

E-mail address: [amina.alshumam@uomosul.edu.iq](mailto:amina.alshumam@uomosul.edu.iq)

DOI: [10.24237/djes.2023.160402](https://doi.org/10.24237/djes.2023.160402)

This work is licensed under a [Creative Commons Attribution 4.0 International License](https://creativecommons.org/licenses/by/4.0/).



## 1. Introduction

Shell footings were introduced in the early 1950s as cost-effective alternatives to traditional flat shallow foundations. Their usage spread extensively across countries such as Mexico, China, and various European nations. In comparison with conventional flat shallow foundations, shell footings require a lesser quantity of construction materials to achieve an equivalent load-carrying capacity due to their thin structural design. The efficiency of shell footings stems from this distinctive design feature. Given their high structural efficiency, this becomes a positive advantage, especially when dealing with heavy structural loads for buildings that are transferred to soil with weak load-bearing capacity. Furthermore, the engineering characteristics of shell footings enable them to perform more efficiently across various scenarios [1].

[2] a study showed that shell footings are cost-effective when used with heavy loads on weak soil. Furthermore, the economic benefits of shell footings become particularly pronounced in tall buildings and industrial structures. However, it is noteworthy that shell footings have not been designed to replace deep foundations.

In a theoretical study conducted by [3] using the PLAXIS software, a comparison was made between the performance of conical shell footings and flat footings with varying dimensions based on different soil types. The study results demonstrated that conical shell footings have a higher load-carrying capacity than their flat counterparts considered in the study, even under the same soil conditions.

[4] conducted a laboratory study on the load-bearing capacity of various types of shallow shell footings (conical shell footings, pyramid shell footings, and flat footings) on sandy soil. The findings revealed that conical and pyramid shell footings exhibited higher load-bearing capacities compared to their traditional flat footing counterparts.

[5] studied models of conical shell footings with different angles. They found that increasing the height-to-radius ratio ( $h/r_2$ ) of

the shell footing from 0.25 to 0.75 makes it 15% stronger. Also, [6] did a study on four models of conical shell footings based on sandy soil. They found that reducing the half-shell angle of the cone increased the load-carrying capacity of the footings and improved the relationship between the load and how much it settled.

A study conducted by [7] aimed to investigate the response of pyramid-shaped shell footings, equivalent hyperbolic paraboloid shell footings, and traditional square footings under the influence of vertical loads at varying embedment depths. These were compared with the square footing model for the same cross-sectional area. The results indicated that the load-carrying capacity of shell footings increases with the rising height-radius ratio (0.3, 0.4, and 0.5) and also with the increase in embedment depth from 0.3 to 0.5. Higher load-carrying capacity values were observed for the shell footings compared to the square footings.

[8] conducted a study on inverted pyramid and upright pyramid shell footings using ANSYS Ver. 15 (2015) software. The study involved comparing the selected types of footings. The study revealed that there is an increase in load-carrying capacity and a decrease in settlement values for inverted pyramid shell footings compared to upright pyramid shell footings. The results also indicated that the contact pressure decreases with increasing both the angle of the shell footing and the thickness of the selected footing sections in the study.

[9] conducted a comparative analytical study regarding the use of different types of conical shell footings, flat circular footings, and theoretical footings using the ANSYS 19.0 software. The results demonstrated that conical shell footings have a higher load-carrying capacity compared to flat circular footings. The load-carrying capacity for the conical shell footing reached 780 KN with a settlement value of 33.872 mm, while the load-carrying capacity for the flat circular footing was 250 KN with a settlement value of 33.465 mm.

In a study by [10] an investigation was carried out regarding stress distribution beneath triangular strip shell footings placed on sandy

soil with three density values (low, medium, and high) and varying embedment depths and edge angles for the shell footing. The results indicated an increase in stress distribution intensity beneath triangular shell footings by reducing the edge angle. The study also revealed that triangular strip shell footings exhibit a higher load-bearing capacity compared to traditional flat footings.

Although the use of this foundation system has a history, studies on it are not widely available and should be further investigated and introduced. Consequently, in this research, a new approach was adopted to study the geotechnical behavior of shell foundations (inverted conical shell footings, inverted pyramidal shell footings, and inverted pentagonal pyramid shell footings) resting on sandy soil. The present study was done using numerical analysis by the software Midas GTS NX. [3].

## 2. Theoretical Modeling Using the Finite Element Method (FEM)

Explaining research chronological, the current study relied on the software package (MIDAS GTS NX) version 1.1. (2021), which is a software tool used for analyzing and modeling various issues in the field of soil

mechanics and foundation engineering (GTS user manual) [11]. In this study, the engineering model for both shell and traditional footing models was established by modeling the soil mass, simulating the rigid volume of soil excavations, and finally simulating the shell footing, as shown in Figure 1. Non-linear material model analysis used to represent the behavior of the soil, as the MIDAS/GTS NX program allows different material models and various boundary conditions. In this study Mohr-Coulomb model were used to model the soil, while the Isotropic-Linear-Elastic model adopted to model the foundations; appropriate boundary conditions were used by restricting the displacement in the bottom side of the x-direction (x) and y-direction (y), the Y direction of the back faces and front faces, the x-direction (x) of the right-faces and left-faces of the geometric model, these constraints allow displacements in the z-direction only. A non-linear material analysis model was selected to represent soil behavior. The specifications and characteristics of this soil, as outlined in Table 1, will be adopted. The properties of the sandy soil were selected based on the study by [12], while the foundation represented by steel and its properties were chosen based on the book by [13].

**Table 1:** presents the properties of both the soil and the footings used in the study

Parameter	Name	Loose sand Soil	Footing	Unit
Material model	Material model	Mohr-Coulomb	Linear-Elastic	
Type of behavior	Drained type	Drained	Non-porous	-
dry unit weight	$\gamma_{dry}$	15.3	80	KN/m <sup>3</sup>
saturated unit weight	$\gamma_{sat}$	15.45	80	KN/m <sup>3</sup>
Elastic modulus	E	30E3	21E7	KN/m <sup>2</sup>
Poisson ratio	$\nu$	0.3	0.18	-----
Cohesion	C	0.001	-	KN/m <sup>2</sup>
Angle of friction	$\phi$	32	-	Deg.

As for the element mesh in the current study, hybrid elements were employed. These elements are formed by combining pyramidal and quadrilateral surfaces on a hexagonal base. Concerning the representation of the soil-foundation interaction surface in the MIDAS/GTS NX program, interface elements available in the MIDAS GTS program were

used. This simulated the material interface properties between the soil and the foundation automatically, based on the assumed virtual thickness factor (tv) and Strength Reduction Factor (R), along with the properties of the soil elements connected to the interface elements. In the current study, the adopted values for these factors are shown in Table 2.

**Table 2:** Interface elements factor

Code	Indication	value
tv	virtual thickness factor	0.05
R	Strength Reduction Factor	0.65

Appropriate boundary conditions for the mesh were defined in this study by constraining displacements in the bottom surface in the x and y directions, as well as the y direction for both the back and front faces and the x direction for the right and left faces of the engineering model, as shown in Figure 2.

For the current study, loads were put on the model in the MIDAS/GTS NX program by making two types of loads and putting them on the selected footings: the self-weight of the soil mass and external loads. The analysis type employed in the current study was construction stage analysis.

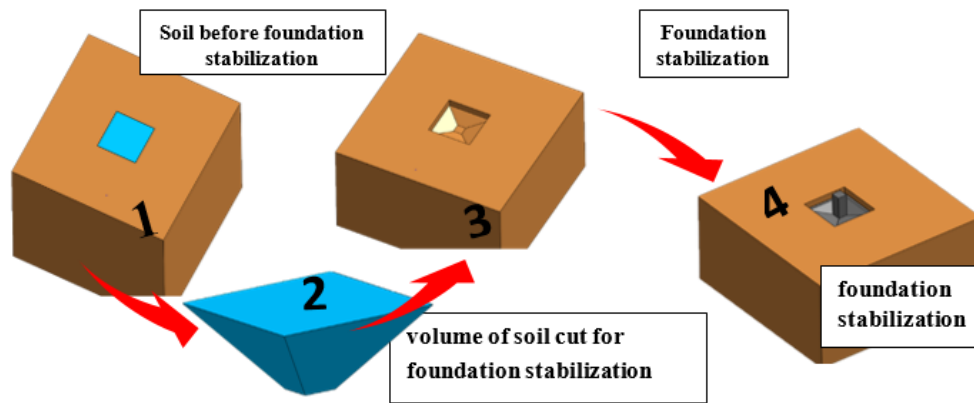


**Figure 1.** Soil excavation modelling using the MIDAS GTS NX software

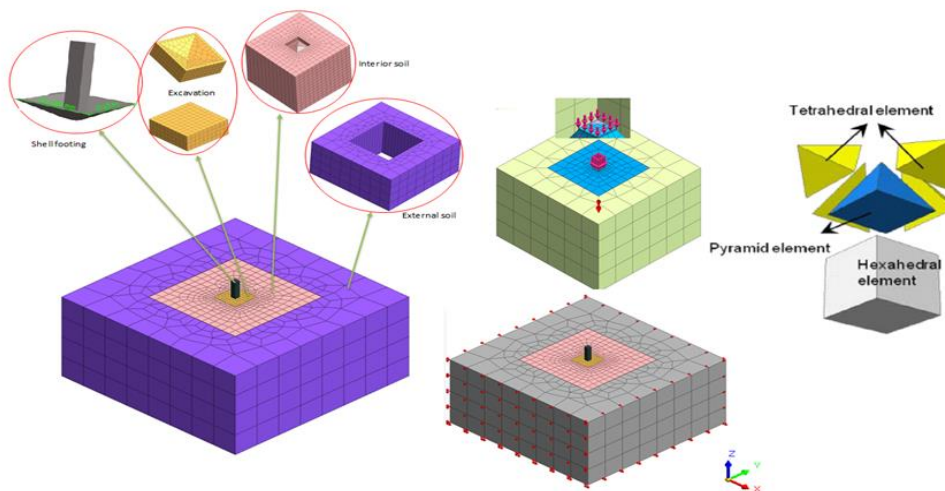


**Figure 2.** Details of the representation of the soil mass and foundation in the program in the MIDAS GTS NX software

### 3. Study parameters

The study parameters encompassed the angle of the shell footing, embedment depth,

and shape (Figure 3 depicts some selected footing sections in the study). The variables were as follows:

- i. Angle of the Shell Footing: Shell footings were investigated at angles of 15°, 30°, and 45°.
- ii. Embedment Depth: Three different embedment depths for the footings were studied (40 cm, 50 cm).
- iii. The thickness of all models is 6 cm.

Based on the selected variables, a total of 24 tests were conducted for both shell and traditional footings. The following key symbols are provided in Table 3 for the footings, angles, and embedment depths to comprehend each trial:

**Table 3:** key symbols for the footings, angles, embedment depths

Key	Indication	Type footing	Key	Indication	Angle	Key	Indication	Depth (cm)
IC		Inverted conical	A		15	Df40		40
IP		Inverted pyramid	B		30	Df50		50
IPP		Inverted Pentagonal Pyramid	C		45			
F_SQU		Flat square						
F_CIR		Flat circle						
F_PP		Flat Pentagonal Pyramid						

Here is an illustrative example of the naming convention: (IP\_C\_DF50) signifies an inverted pyramid shell footing with an angle of 45° and an embedment depth of 50 cm.

Following the same pattern, labels were assigned to the rest of the cases as outlined in Table 4.

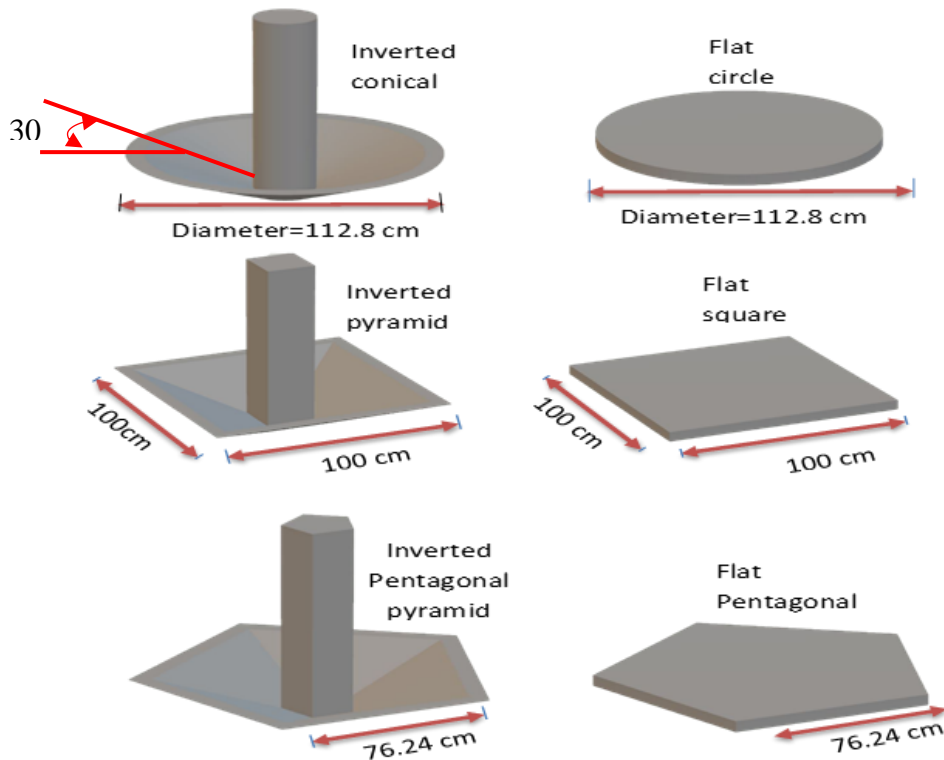


**Table 4:** Run names and numbers

No.	Type footing	Model	Shell angle	Embedment depth
1	I-Conical	IC-A- Df40	15	40
2	I-Conical	IC-A- Df50	15	50
3	I-Conical	IC-B- Df40	30	40
4	I-Conical	IC-B- Df50	30	50
5	I-Conical	IC-C- Df40	45	40
6	I-Conical	IC-C- Df50	45	50

7	I-Pyramid	IP-A- Df40	15	40
8	I-Pyramid	IP-A- Df50	15	50
9	I-Pyramid	IP-B- Df40	30	40
10	I-Pyramid	IP-B- Df50	30	50
11	I-Pyramid	IP-C- Df40	45	40
12	I-Pyramid	IP-C- Df50	45	50
13	I-Pentagonal Pyramid	IPP-A- Df40	15	40
14	I-Pentagonal Pyramid	IPP-A- Df50	15	50
15	I-Pentagonal Pyramid	IPP-B- Df40	30	40
16	I-Pentagonal Pyramid	IPP-B- Df50	30	50
17	I-Pentagonal Pyramid	IPP-C- Df40	45	40
18	I-Pentagonal Pyramid	IPP-C- Df50	45	50
19	Flat square	F_SQU. _DF40	-	40
20	Flat square	F_SQU. _DF50	-	50
21	Flat circle	F_CIR. _DF40	-	40
22	Flat circle	F_CIR. _DF50	-	50
23	Flat Pentagonal Pyramid	F_PP_DF40	-	40
24	Flat Pentagonal Pyramid	F_PP_DF50	-	50

#### 4. Results

The study investigated the effect of varying the slope angle of the side of the inverted shell footing for three angles (15°, 30°, and 45°) and the embedment depth for two values (40 cm and 50 cm) on the change in settlement values due to applied load for the six sections of the selected footings (three sections for the shell footing and three sections for the traditional flat footings). Additionally, the efficiency factor of the shell footing was determined using Equation (1), as well as the settlement improvement factor according to Equation (2) [14]. The results obtained are presented as follows:

$$\eta = \frac{Q_{us} - Q_{uf}}{Q_{uf}} \times 100\% \quad (1)$$

$$F_a = \frac{\delta_u \gamma A_b}{Q_u} \quad (2)$$

$\eta$ : shell efficiency,  $F_a$ : settlement factor,  $Q_{uf}$ : flat footing ultimate load,  $Q_u$ : ultimate load,  $Q_{us}$ : shell footing ultimate load,  $\gamma$ : soil unit weight,  $\delta_u$ : settlement at ultimate load,  $A_b$ : area of the footing in the horizontal projection.

##### 4.1 The load-settlement relationship for all footing models

The maximum load-carrying capacity was determined for all selected footing sections at a settlement value of 25 mm according to [4]. Figures (4, 5, and 6) illustrate the load-settlement curves for the shell footing models. The results indicated that shell footings have a greater load-carrying capacity compared to traditional flat footings.

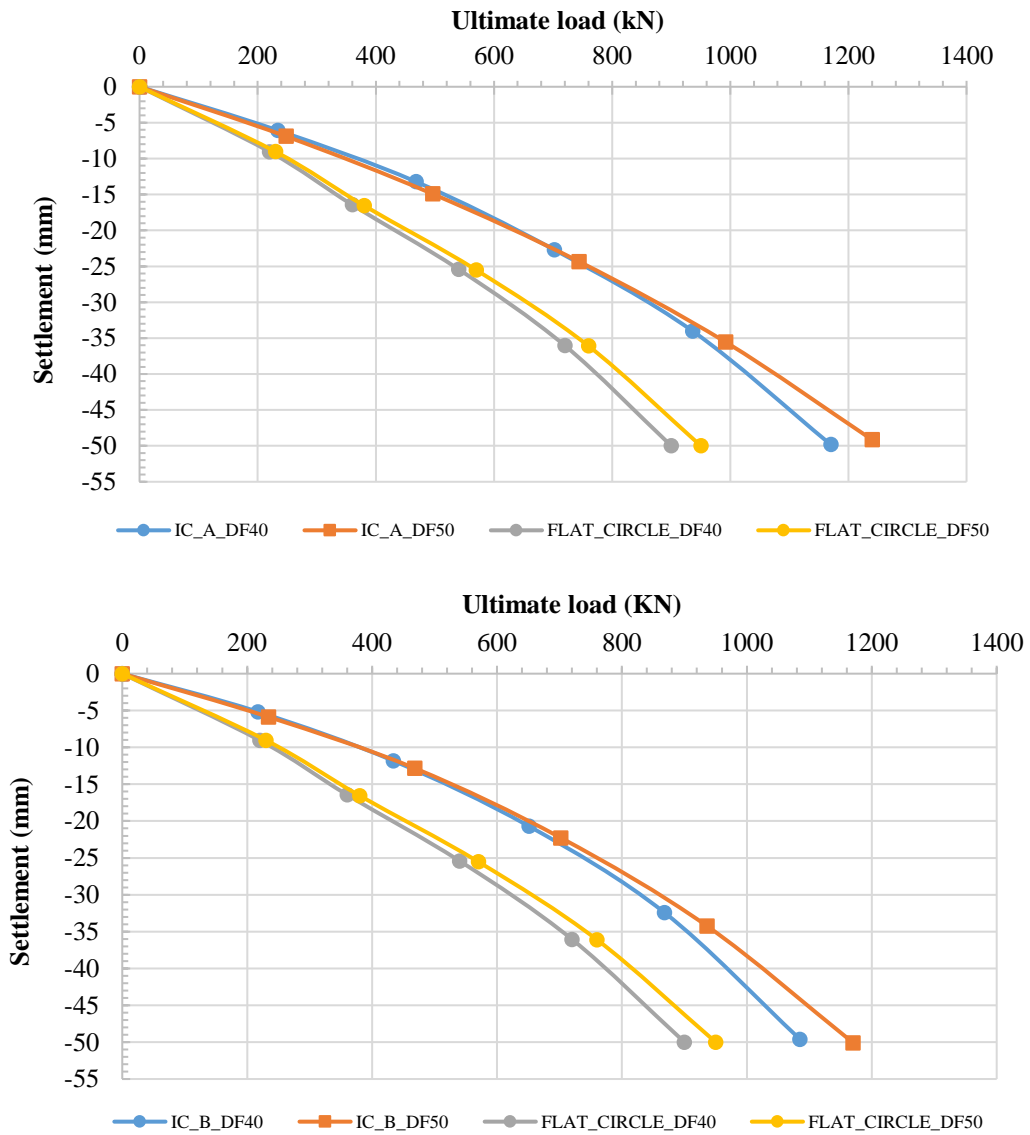
The results demonstrated that inverted pyramid shell footings have a higher load-carrying capacity compared to inverted conical and inverted pyramid pentagonal shell footings. Also, the results showed that inverted pyramid pentagonal shell footings have a higher load-carrying capacity than inverted conical shell footings. Furthermore, the results indicated that the settlement values of inverted shell footings are lower than those of traditional flat footings.

When using the tangent method to determine settlement values, sketch two tangents. The first tangent represents the curve's starting point, while the second represents the finishing point. The settlement is determined by the maximum load that a foundation can support when two tangent lines meet [15]. The results indicate that the settlement values of inverted shell footings are lower than the settlement values of traditional flat footings.

Through the load-settlement relationship in Figures (4, 5, and 6), as well as the deformation shape in the vertical direction (displacement) occurring in the foundations with the selected soil mass for the study after completing the

loading in the program, as shown in Figures (7 and 8), it can be concluded that the type of

failure is local shear failure, and this type of failure occurs in weak soil.



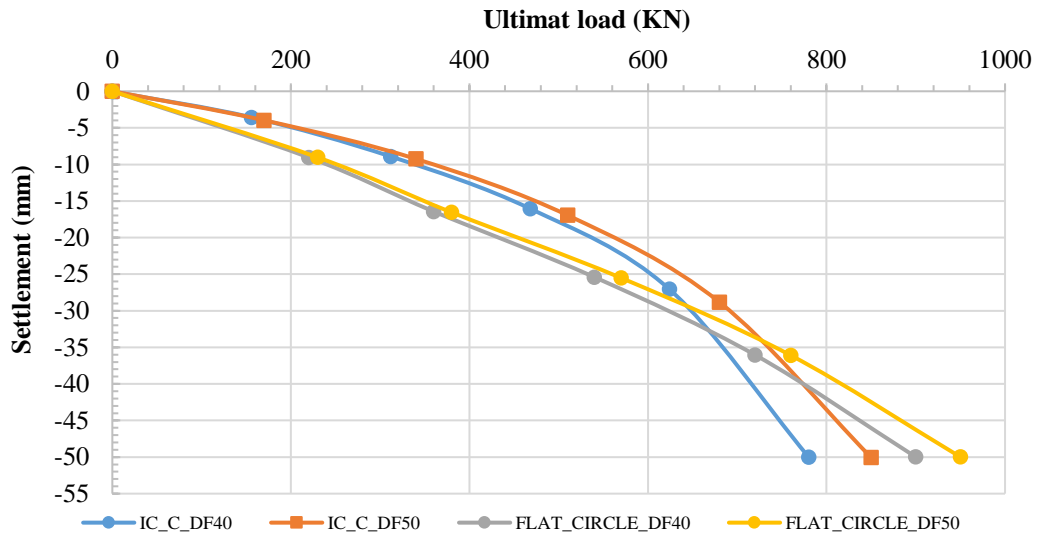
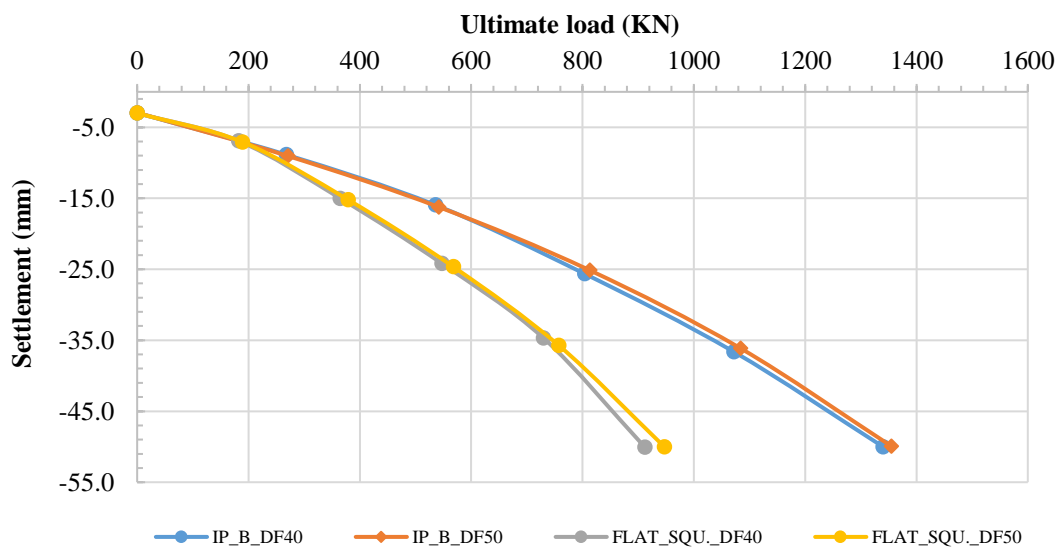
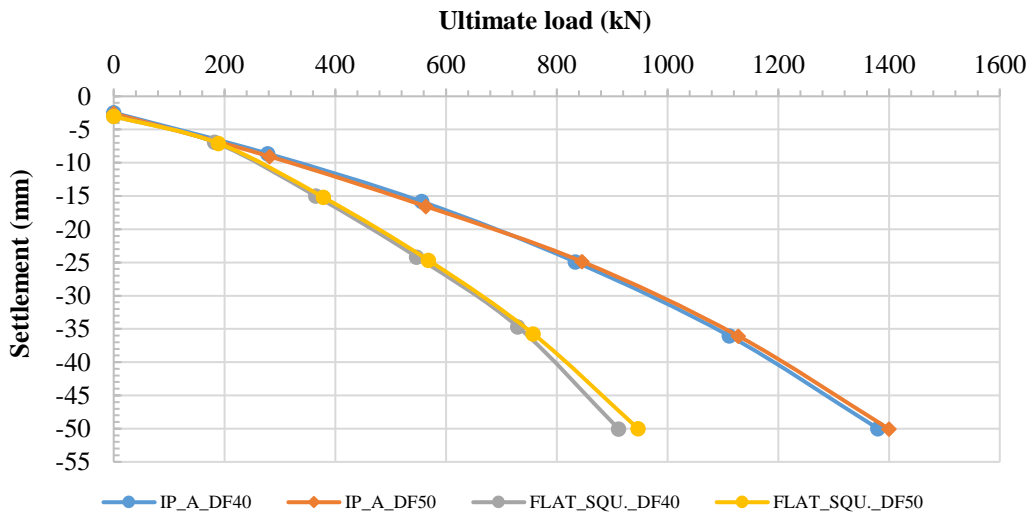


Figure 4. Load-settlement relationship for the conical shell footings





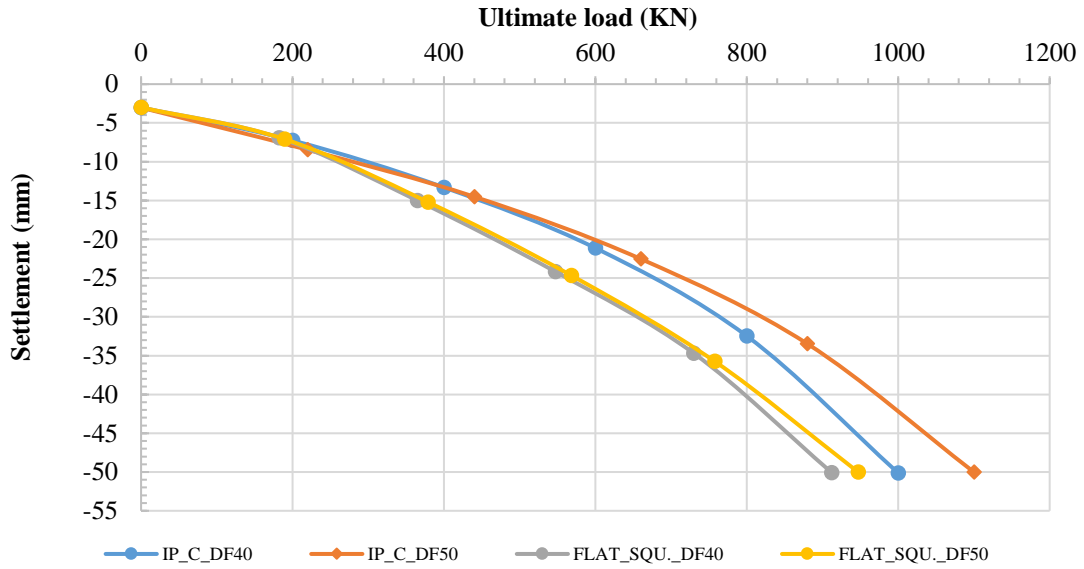
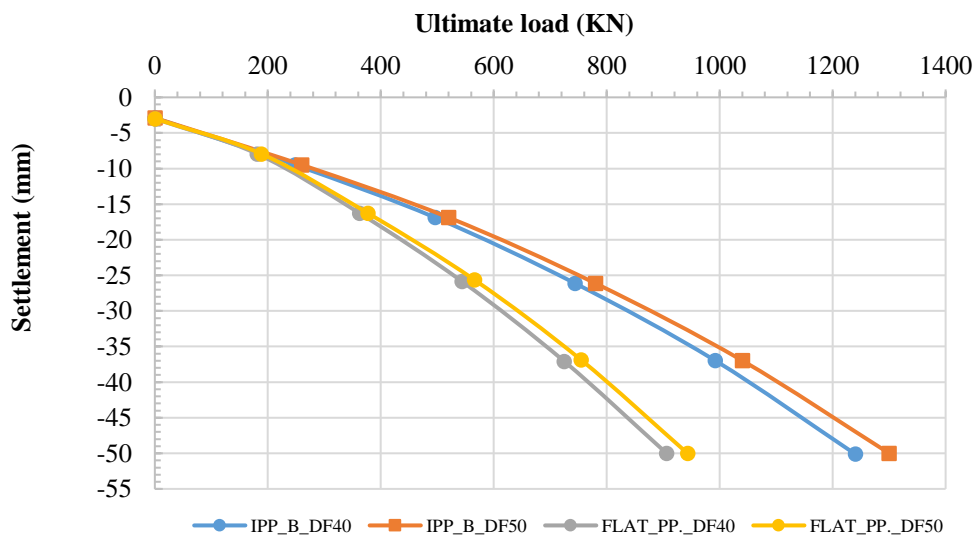
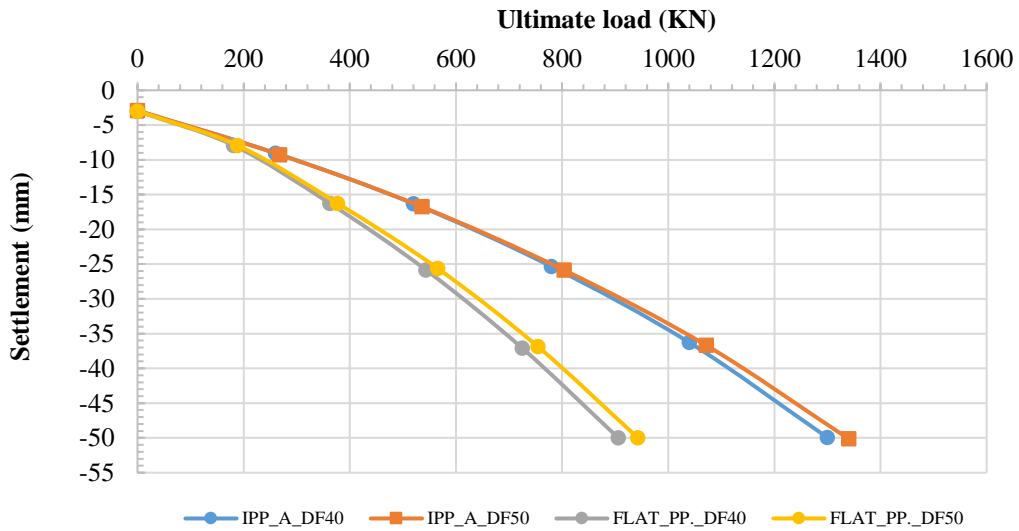


Figure 5. Load-settlement relationship for pyramid shell footings



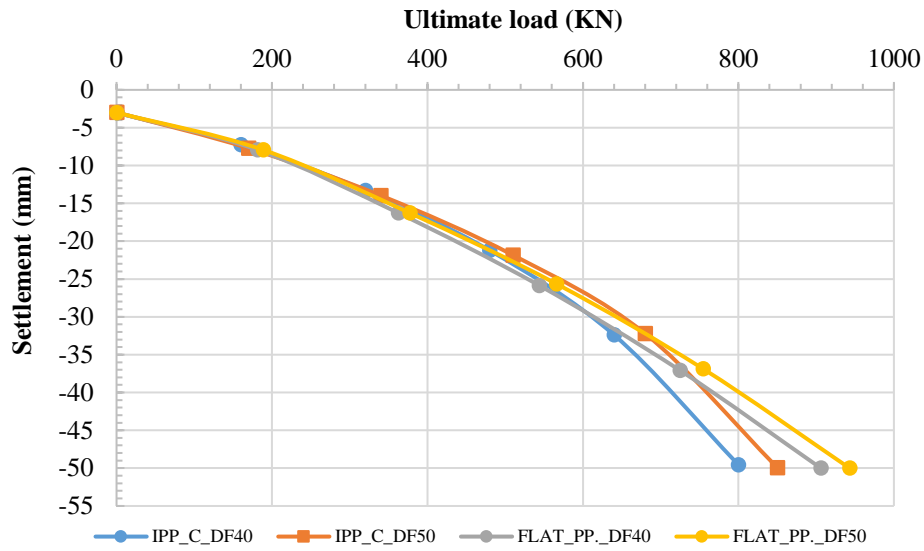


Figure 6. Load-settlement relationship for pyramid pentagonal shell footings

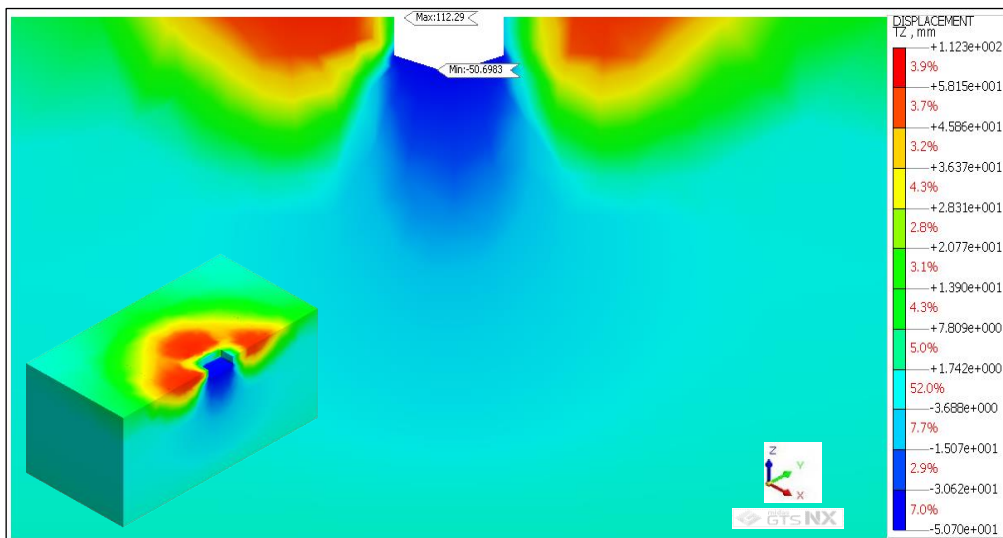


Figure 7. Vertical deformation of the shell foundation (IP\_A\_DF40)

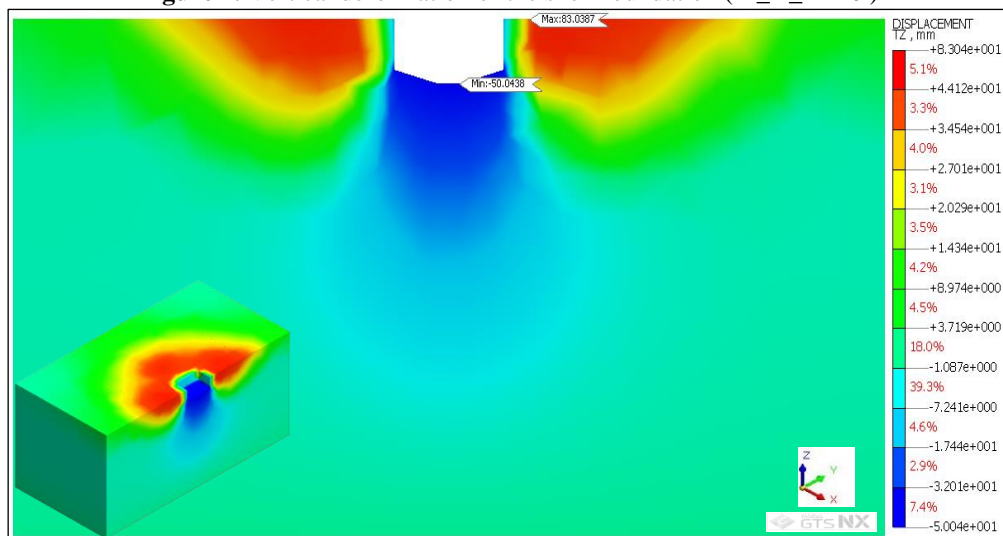
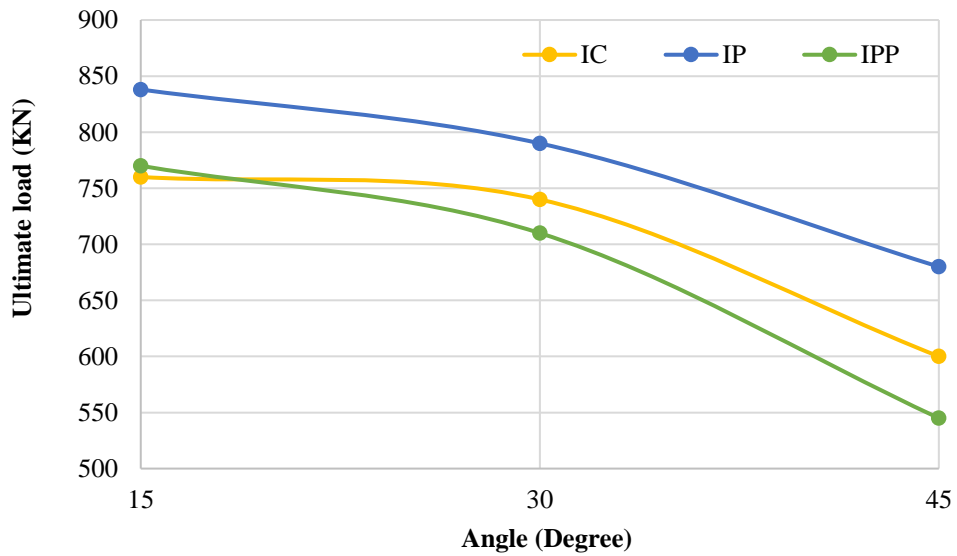


Figure 8. Vertical deformation of the shell foundation (IP\_A\_DF50)

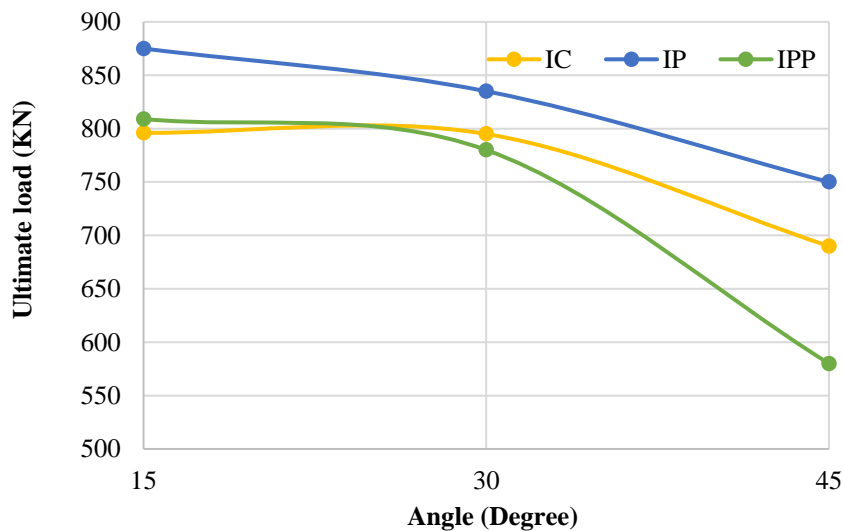
#### 4.2 The effect of the shell footing angle

The study used inverted shell footings with three different side slope angles (15°, 30°, and 45°). Figure 9 shows how these angles changed the way the loads settled on the footings. In general, it can be observed that inverted shell footings show a decreasing load-carrying capacity with an increase in the angle of the side slope of the shell footing, This confirms the findings of the researcher [8,16]. This is because with an increase in the angle, the ratio of the foundation height to width increases.

This makes the foundation pointed, penetrating the soil easily, and thus reducing the load-carrying capacity. The load-carrying capacity of foundations at an angle of 15° to 30° is higher than that of traditional foundations. The load-carrying capacity is higher than 48.3% and 39.8% for the pyramidal shell foundation at an angle of 15° to 30°, respectively. The only foundation whose load-carrying capacity dropped to the level of traditional foundations was the one at an angle of 45°, For the same reason mentioned above.



a)



b)

**Figure 9.** Effect of angle on conical, pyramidal, and pyramidal pentagonal shell footings a) DF = 40 cm; b) DF = 50 cm)

### 4.3 The effect of embedment depth

Two different embedment depths (40 cm and 50 cm) were used to study the effect of embedment depth on the load-settlement behavior of the chosen shell footing. As illustrated in Table 5, the load-carrying capacity values of the chosen foundations were analyzed at different embedment depths. The results showed a general increase in load-carrying capacity values with an increase in the embedment depth for the selected depths in the study. When the embedment depth varies from 40 cm to 50 cm for the inverted conical shell foundation. At 15 degrees, 30 degrees, and 45 degrees of side slope, the load-carrying capacity increased by 0.65%, 2.97 percent, and 5.83 percent, respectively. When the embedment depth was changed from 40 to 50 cm in the case of the inverted pyramidal shell foundation, the load-carrying capacity went up by 1.43 percent at 15 degrees of slope, 3.71 percent at 30 degrees of slope, and 5.14 percent at 45 degrees of slope. On the other hand, for the inverted pyramidal pentagonal shell footing, the depth of embedment had a significant effect on load-carrying capacity. Changing the embedment depth from 40 cm to 50 cm led to an increase in load-carrying capacity of 1.29%, 5.63%, and 4.58% for side slope angles of 15°, 30°, and 45°, respectively.

### 4.4 The effect of embedment depth

Two different embedment depths (40 cm and 50 cm) were used to study the effect of embedment depth on the load-settlement behavior of the chosen shell footing. As illustrated in Table 5, the load-carrying capacity values of the chosen foundations were analyzed at different embedment depths. The results showed a general increase in load-carrying capacity values with an increase in the embedment depth for the selected depths in the study. When the embedment depth varies from 40 cm to 50 cm for the inverted conical shell foundation. At 15 degrees, 30 degrees, and 45 degrees of side slope, the load-carrying capacity increased by 0.65%, 2.97 percent, and 5.83 percent, respectively. When the embedment depth was changed from 40 to 50

cm in the case of the inverted pyramidal shell foundation, the load-carrying capacity went up by 1.43 percent at 15 degrees of slope, 3.71 percent at 30 degrees of slope, and 5.14 percent at 45 degrees of slope. On the other hand, for the inverted pyramidal pentagonal shell footing, the depth of embedment had a significant effect on load-carrying capacity. Changing the embedment depth from 40 cm to 50 cm led to an increase in load-carrying capacity of 1.29%, 5.63%, and 4.58% for side slope angles of 15°, 30°, and 45°, respectively.

**Table 5:** Load-carrying capacity values of the selected footing in the study at different embedment depths

Type Footing	Depth	
	DF40	DF50
	Ultimate load (KN)	
IC-A	760	765
IC-B	740	762
IC-C	600	635
IP-A	838	850
IP-B	790	820
IP-C	680	715
IPP-A	770	780
IPP-B	710	750
IPP-C	545	570
FLAT_CIR	544	560
FLAT_SQU.	565	580
FLAT_PP	530	555

The shell efficiency factor ( $\eta$ ) was calculated according Equation (1), which describes the relationship between the maximum load-carrying capacity of the shell footing and the load-carrying capacity of the flat footing. Additionally, the settlement improvement factor was calculated using Equation (2).

The results showed that the shell efficiency factor ( $\eta$ ) for the inverted pyramid footing with an angle of 15°–30° was higher than the other selected footing types, with values of (48.3%, 46.5%) for the footing types IP\_A\_DF40 and IP\_A\_DF50, respectively. This is illustrated in Figure 10.

Equation (2) using to determine the settlement improvement factor ( $F_a$ ), the results showed that the inverted pyramid footing with

an angle of  $15^{\circ}$ – $30^{\circ}$  had a lower settlement improvement factor than the other footing types used in the study. The settlement improvement factors for the selected footing types IP\_A\_DF40 and IP\_A\_DF50 were ( $5.07 \times 10^{-4}$ ,  $5 \times 10^{-4}$ ) respectively. This is illustrated in Figure 11.

It's noteworthy that a decrease in the settlement improvement factor indicates better

performance for the shell foundation in distributing and transferring loads with less settlement. Thus, it enhances the settlement property. In other words, the lower the value of this factor, the lower the settlement, and the higher the load-carrying capacity.

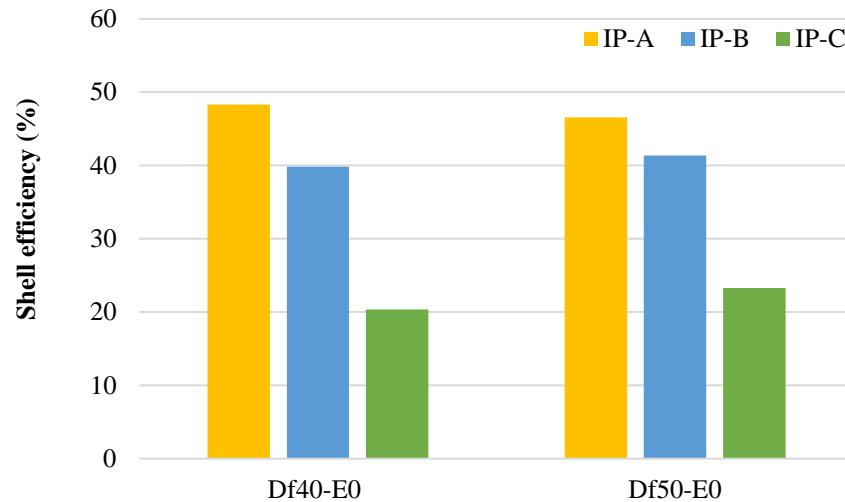


**Figure 10.** Efficiency of inverted pyramid shell footing

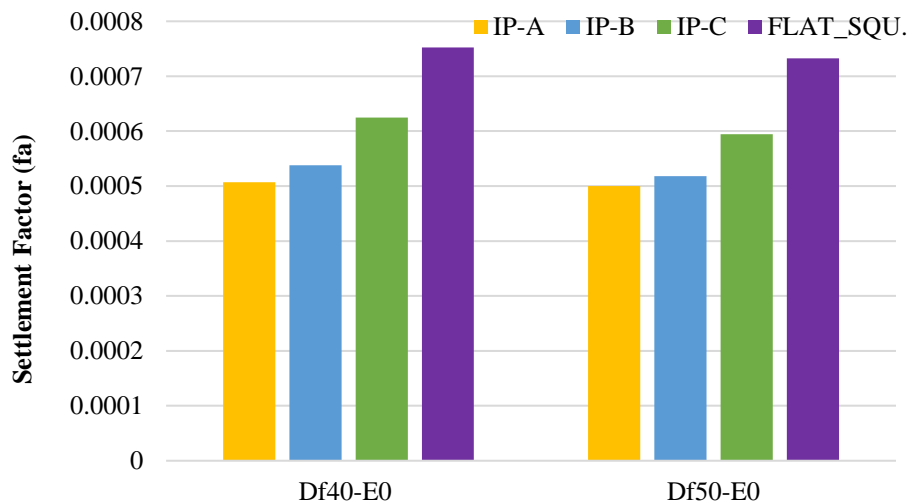


**Figure 11.** Settlement improvement factor for inverted pyramid shell footing

## 5. Conclusions

Based on the theoretical modelling and in light of the results obtained regarding the selected footing sections in the study, and based on the analysis of the results, the following conclusions can be obtaining:

1. In general, the selected inverted shell footing sections in the study have a higher load-carrying capacity if it compared with traditional flat foundations.
2. Inverted shell foundations within the range of side slope angles  $15^{\circ}$ – $30^{\circ}$  exhibit higher load-carrying capacity than

traditional flat foundations. The inverted pyramid shell foundation with a side slope angle of  $15^\circ$  (IP-A-Df40-E0) has a load-carrying capacity of 838 KN.

3. Increasing of the embedment depth is effective in increasing the load-carrying capacity of inverted shell foundations.
4. In general, inverted shell foundations exhibit good efficiency compared to traditional foundations. The inverted pyramid shell footing with a side slope angle of  $15^\circ$ – $30^\circ$  has a higher efficiency compared to other footings, with values of (48.3%, and 46.5%) for the footing types (IP\_A\_DF40, IP\_A\_DF50), respectively.
5. The settlement improvement factor of inverted shell footing is relatively low. The inverted pyramid shell footing with a side slope angle of  $15^\circ$ – $30^\circ$  has lower values compared to other footings, with values of ( $5.07 \times 10^{-4}$ ,  $5 \times 10^{-4}$ ) for the footing types (IP\_A\_DF40, IP\_A\_DF50), respectively.

## References

- [1] Ou, Guangjun. "Lateral Force Resistance for Shell Foundation." Ph.D. diss., Concordia University, 2021.
- [2] Kurian, N. P. "Economy of hyperbolic paraboloidal shell footings." *Geotech Eng* 8 (1977): 53-59.
- [3] Chekol, E. T., & Seged, H. "A study on the design and advantage of conical type shell foundation using analytical and FEM." Addis Ababa University (2009).
- [4] Fernando, N., Sendanayake, E., Sendanayake, D., & De Silva, N. "The experimental investigation of failure mechanism and bearing capacity of different types of shallow foundations." *Civil Engineering Research for Industry*, Department of Civil Engineering, University of Moratuwa (2011).
- [5] Fattah, M. Y., Waryosh, W. A., & Al-Hamdani, M. A. "Experimental and theoretical studies on bearing capacity of conical shell foundations composed of reactive powder concrete." *Acta Geodynamica et Geomaterialia* 12, no. 4 (2015): 411-426.
- [6] Ramesh, M., & Joy, B. M. "Experimental study on conical shell footing." *Int J Eng Res Technol* (2015).
- [7] Ab Rahman, A. R. "Performance of physical shell foundation model under axial loading." Ph.D. diss., Universiti Tun Hussein Onn Malaysia, 2016.
- [8] Sidqi, R., & Mahmood, M. N. "Investigating the Nonlinear Performance of Reinforced Concrete Shell Foundations." In *IOP Conference Series: Materials Science and Engineering*, vol. 978, no. 1, p. 012050. IOP Publishing, 2020.
- [9] Lamy, T., and M. K. Sheeja. "Analytical Assessment on the Behaviour of Conical Shell Foundation." In *Proceedings of SECON 2020: Structural Engineering and Construction Management* 4, pp. 307-316. Springer International Publishing, 2021.
- [10] Ansari, A. "Stresses in Soil Beneath Triangular Shell Foundations." Ph.D. diss., Concordia University, 2022.
- [11] Midas GTS NX-Geotechnical Analysis System New Experience, version 1.1. (2021). Bundanggu, Seongnam-si, gyeonggi-do, Korea: midas information Co., Ltd. GTS Tutorial, <https://www.midasuser.com/>.
- [12] Sajedi, K., Bolouri Bazaz, J., & Rezaee Pajand, M. "Elastic-Plastic Analysis of Inverted Folded Shell Strip Foundation on Sandy Soil." *Journal of Civil and Environmental Engineering* 47, no. 89 (2018): 15-26.
- [13] Bowles, J. E. "Foundation analysis and design". 1988. McGraw-Hill, 5th edition.
- [14] Hanna, A., & Abdel-Rahman, M. "Experimental investigation of shell foundations on dry sand." *Canadian Geotechnical Journal* 35, no. 5 (1998): 847-857.
- [15] Ahmad, H., Hoseini, M. H., Mahboubi, A., Noorzad, A., & Zamanian, M. "Effect of sheet pile wall on the load-settlement behaviour of square footing nearby excavation." *Geomechanics and Geoenvironment* 18, no. 2 (2023): 149-167.
- [16] Sajedi, K., & Bolouri Bazzaz, J. "Edged Inverted Folded Plate Shell Strip Foundation Bearing Capacity Comparison with strip footing on Sandy Soil." *Journal of Rehabilitation in Civil Engineering* 10, no. 3 (2022): 121-140.